

# Morphology Selection of Nanoparticle Dispersions by Polymer Media

JAEUP U. KIM <sup>1</sup> and BEN O'SHAUGHNESSY <sup>2</sup>

<sup>1</sup> Department of Physics, Columbia University, New York, NY 10027

<sup>2</sup> Department of Chemical Engineering, Columbia University, New York, NY 10027

Submitted To: *Physical Review Letters*

## ABSTRACT

Designable media can control properties of nanocomposite materials by spatially organizing nanoparticles. Here we theoretically study particle organization by ultrathin polymer films of grafted chains (“brushes”). Polymer-soluble nanoparticles smaller than a brush-determined threshold disperse in the film to a depth scaling inversely with particle volume. In the polymer-insoluble case, aggregation is directed: provided particles are non-wetting at the film surface, the brush stabilizes the dispersion and selects its final morphology of giant elongated aggregates with a brush-selected width.

PACS numbers:

82.35.Np	(Nanoparticles in polymers)
68.08.-p	(Liquid-solid interfaces: Wetting)
82.35.Jk	(Copolymers, phase transitions, structure)

The prospect of a new generation of materials and devices based on the assembly of nanoparticles into spatially extended 2D and 3D arrangements is a major driving force in the rapidly emerging field of nanoscale research [1,2]. Nanoparticles, the “designer molecules” governing the macroscopic behavior of these novel materials, can be constructed according to a vast range of design principles, promising unprecedented tuning of material properties. Both for technology and for fundamental research in condensed matter physics, the implications are far-reaching.

This letter addresses a major challenge in the field: how to spatially organize the nanoparticles. The interparticle *medium* plays a crucial role in this regard, and one would like to “design” media to achieve different spatial arrangements leading to different interparticle couplings and entirely different macroscopic properties. Much recent research has examined polymeric media spontaneously forming nanostructured phases as templates for particle organization [1,2,3,4]. Moreover, polymer-particle composites are often conveniently processable with important implications for thin film and other technologies [2,5,6].

In this letter we develop a systematic theory of ultrathin polymer films as organizing media to achieve 2D nanoparticle arrangements. The latter are central to information storage media applications and of fundamental importance to 2D electronic phenomena. We are directly motivated by recent studies [2,5] of metallic and semiconducting nanoparticles in films of end-tethered polymer chains forming “polymer brushes,” and in diblock copolymer materials whose lamellae offer a similarly 2D brush-like environment [3,6]. A major objective is that this work offer guidance to such experiments by identifying the key physical variables to achieve nanoparticle dispersions and control morphology.

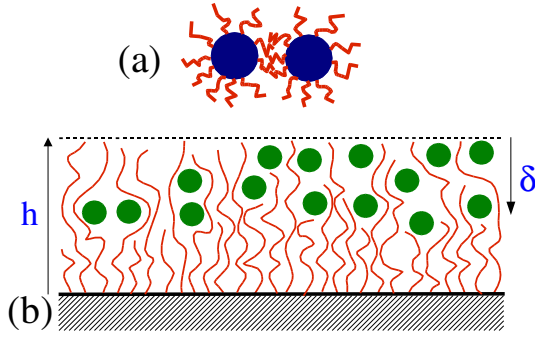


Figure 1: (a) Typical nanoparticles comprise inorganic cores of several  $nm$ , plus stabilizing oligomeric coronas for compatibilization with polymer medium. (b) Schematic of polymer film containing nanoparticles in contact with air. Chains are grafted to substrate, forming a stretched “brush” of height  $h$  at large grafting density  $\sigma$ .

Given a nanoparticle-containing film of substrate-grafted polymer chains of  $N$  units at grafting density  $\sigma$  (fig. 1 (b)) in contact with air, we will see there are two distinct classes of behavior depending on whether the particles are (A) soluble or (B) insoluble in the free polymer medium (ungrafted chains). Our principle conclusions are as follows:

(A) For **polymer-soluble** particles (well-compatibilized) their size  $b$  is crucial: (i) Sufficiently small particles disperse freely within the polymer brush film. (ii) Above a threshold size  $b^*$ , equilibrium particle penetration is limited to a depth  $\delta$  and the film has a loading capacity  $\phi_{\max}$ . Both  $\delta$  and the maximum particle density  $\phi_{\max}$  scale inversely with particle volume  $b^3$ . (iii) Particles larger than a second threshold  $b_{\max} \approx (N/\sigma)^{1/4}$  cannot penetrate the film.

(B) **Polymer-insoluble** particles tend to aggregate in the polymer film, of course. This aggregation is *directed* by the polymer brush: (i) The brush imposes a severe free energy

penalty for aggregate growth in two lateral directions simultaneously (parallel to substrate): large *anisotropic* aggregates tend to form, elongated in one lateral direction. (ii) As growth continues, aggregates are expelled towards the brush-air interface and the final state depends on the polymer-nanoparticle-air interfacial tensions. If the nanoparticles tend to wet the polymer film surface, they will spread to form a near-monolayer. In the non-wetting case, growth is ultimately arrested and the final morphology consists in large elongated aggregates, embedded in the film, whose width is selected by the brush.

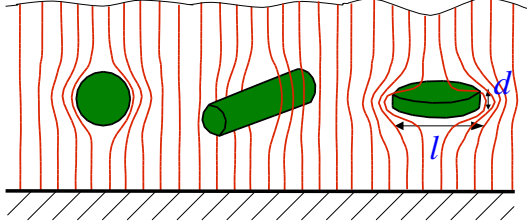


Figure 2: The degree an inclusion disrupts a polymer brush depends strongly on shape. To within prefactors, the free energy costs  $\Delta F$  for a cylinder and a sphere of the same volume are equal because chain distortion is determined by cylinder radius rather than its length. But chain configurations are far more strongly distorted by a disk and  $\Delta F$  is much higher, increased by the disk aspect ratio  $l/d$ .

Before proceeding, a few remarks concerning these conclusions may be helpful. Inevitably, polymer-insoluble nanoparticles will eventually phase separate if thermodynamic equilibrium is accessible. Thus the experimental procedure must not only forcibly introduce the particles into the polymer film, but thereafter their eventual expulsion and phase separation must be prevented by physical constraint. (Alternatively, kinetics may naturally intercede by inhibiting particle fluidization in the air medium.) Our conclusions for case (B) have assumed this, and this turns out to be the most interesting case: provided the particles are non-wetting on the film surface, the brush *stabilizes* the nanocomposite and *selects the morphology* of giant anisotropic nanoparticle aggregates with a selected lateral dimension. The physical origin of these effects is that aggregates extended simultaneously in two lateral directions impose radical distortions on the brush chain configurations (see fig. 2), whereas chains are relatively undistorted by an aggregate elongated in only one direction, around which they can “flow” by taking the shortest route. This leads to a much lower free energy cost.

For the remainder of this letter we briefly outline our calculations leading to these conclusions; we then compare with experiment, and we finish by proposing optimal future experimental strategies based on this work.

In typical grafted polymer films, chain end anchoring is achieved by attaching an end block chemically similar to the substrate [5]. It is well known that as grafting density increases brush height  $h$  increases (see fig. 1 (b)) due to incompressibility,  $h = \sigma N$ , and chains are forced to stretch away from the substrate. Since a Gaussian chain has stretching energy  $(1/2) h^2/N$  [7], this leads to a brush stretching energy density or “pressure”  $P_0 = (1/2)(h/N)^2 = (1/2)\sigma^2$ . (Units are chosen so both  $kT$  and the size of one monomer unit are unity, so the volume of one chain is  $N$ .)

Now suppose nanoparticles are forced into such a brush (see fig. 1 (a)); typically these are surface-stabilized metallic, metal oxide or semiconductor nanocrystals [2,3,6]. We first

consider polymer-soluble particles, case (A). To determine nanoparticle density distributions  $\phi_{nano}(\mathbf{r})$  within the brush, our starting point is the following brush free energy as a function of chain configurations  $\mathbf{R}(n, \rho)$  ( $n$  is the monomer label,  $0 \leq n \leq N$ ,  $\mathbf{r} \equiv (x, y, z)$  with  $z$  orthogonal to substrate):

$$F = \int d\rho g(\rho) \frac{3}{2} \int_0^N dn \left( \frac{\partial \mathbf{R}}{\partial n} \right)^2 + \int d\mathbf{r} P(\mathbf{r}) (\phi_{pol}(\mathbf{r}) + \phi_{nano}(\mathbf{r}) - 1) + F_{nano}[\phi_{nano}] \quad (1)$$

where  $\phi_{pol}(\mathbf{r}) \equiv \int d\rho g(\rho) \int_0^N dn \delta(\mathbf{r} - \mathbf{R}(n, \rho))$  is the polymer density and  $g(\rho)$  is the distribution of chain end locations  $\rho$ ,  $\mathbf{R}(0, \rho) \equiv \rho$ . The first term represents chain stretching free energy [8], the pressure-like field  $P(\mathbf{r})$  enforces incompressibility and  $F_{nano}$  describes interactions involving nanoparticles.

Now if one deletes the nanoparticle terms, this gives the free energy considered by Semenov for the pure non-solvated brush [8]. Semenov found that in the free-energetically favored brush configuration chain ends are in fact distributed throughout the brush, i.e. the “Alexander-de Gennes” picture in which all ends lie at height  $h$  is wrong. Correspondingly, the pressure field is non-uniform and quadratic,  $P(z) = CP_0(1 - z^2/h^2)$  where  $C = 3\pi^2/4$ .

Extending Semenov’s analysis, we minimize  $F$  with respect to both polymer plus nanoparticle fields. At moderate volume fractions  $F_{nano} \simeq \int d\mathbf{r} (\phi_{nano}/b^3) \ln(\phi_{nano}/e)$  is dominated by translational entropy and we find in equilibrium

$$\phi_{nano}(z) = \phi_{nano}(h) e^{-P(z)b^3} \quad (2)$$

where the pressure field remains quadratic but the substrate pressure and brush height are increased. Noting the pressure vanishes at the brush surface  $z = h$ , and is approximately linear for small depths, we write  $\phi_{nano}(z) \sim e^{-(h-z)/\delta}$  where  $\delta \equiv h(b^*/b)^3$  and  $b^* \approx (N/h)^{2/3} = 1/\sigma^{2/3}$ . Thus for  $b \gg b^*$  the penetration depth  $\delta \sim 1/b^3$  is much less than the full brush height. It decreases with increasing particle size until  $\delta = b$  defines the maximum sized particle  $b = b_{max} \approx (N/\sigma)^{1/4}$  which can enter the brush. In the partial penetration regime,  $b^* < b < b_{max}$ , the maximum particle volume fraction is  $\phi_{max} = \delta/h \sim 1/b^3$ . Above this level, excess nanoparticles are expelled outside [9].

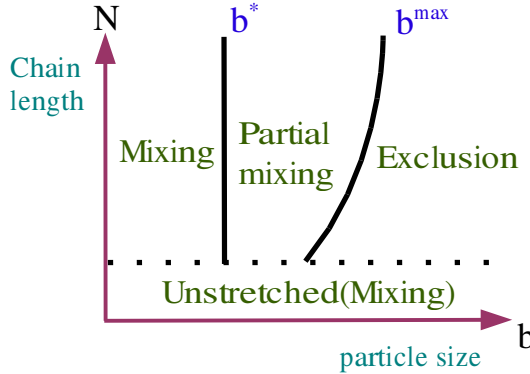


Figure 3: **Polymer-soluble nanoparticles (case (A)):** phase diagram as a function of particle size ( $b$ ) and polymer chain length ( $N$ ). Particles smaller than  $b^*$  mix freely in the film while those larger than  $b_{max} \sim N^{1/4}$  are excluded. In the intermediate regime,  $b^* < b < b_{max}$ , partial film penetration occurs to a depth  $\delta \sim 1/b^3$  with loading capacity  $\phi_{max} = \delta/h \sim 1/b^3$ .

These results are represented in fig. 3. Their physical origin is clear. Because of Semenov’s chain end relaxation effect, the edge of the brush is much softer than elsewhere and the pressure profile increases monotonically as one moves away from the free brush surface.

This provides a “buoyancy” force on any inclusion, tending to push particles to the brush surface. Mixing entropy opposes this, and the balance leads to the density field of eq. (2). The penetration depth  $\delta$  is obtained by balancing the entropy, of order  $kT$ , with  $P(\delta)b^3$  which is the particle’s chain stretching energy penalty at depth  $\delta$ .

Let us now turn to case (B), nanoparticles insoluble in the polymer medium, i.e. the nanoparticle-polymer interfacial tension  $\gamma_{np}$  (see below) exceeds a critical (positive) value. After being forced into the brush, van der Waals attractions coalesce them into increasingly big aggregates [5]. Unchecked, phase separation would result. Now to understand how the brush may intervene, we must go beyond the analysis above which produced density profiles homogeneous in the lateral directions  $(x, y)$ . This is meaningful only for nanoinclusions which can be treated as fluid-like perturbations, i.e. those smaller than the brush “blob” size  $\xi$ . This is the scale over which a brush chain’s statistics are of unperturbed Gaussian character, while on larger scales the global stretching is felt [7]. When large aggregates grow ( $b > \xi$ ) the brush is strongly disrupted locally and  $(x, y)$  symmetry is broken. From a theoretical standpoint, the problem is intrinsically non-perturbative. Amongst previous works addressing this problem [10,11], an important contribution was due to Williams and Pincus [12] who proved that an object in a strongly stretched brush is formally analogous to irrotational steady state inviscid flow past the same object. Polymer configurations map to flow streamlines, and the brush energy equals the fluid kinetic energy [12].

Exploiting this analogy, by using flow solutions past various objects [13] we have calculated the brush energy cost  $\Delta F$  for nanoparticles to form aggregates of different sizes and shapes. (see fig. 2) We find that momentum conservation in the hydrodynamic analogy translates to the statement that for a given aggregate volume  $\Omega$  there is a baseline free energy cost of exactly  $2P_0\Omega$ . Additional free energy cost depends on aggregate shape: we find  $\Delta F = (5/2)P_0\Omega$  and  $3P_0\Omega$  for, respectively, spheres and for long cylinders parallel to the substrate. Most interestingly, *disk-shaped* aggregates of diameter  $l$  and thickness  $d$  are much more costly:  $\Delta F = (4/3\pi)P_0\Omega(l/d)$  is dominated by the aspect ratio factor,  $l/d \gg 1$ .

While helpful, these results are not quite conclusive since the hydrodynamic analogy applies only to the simplified “Alexander-de Gennes” brush [12]. How does chain end-annealing modify these findings? To answer this, we have established rigorous bounds on  $\Delta F$  for an inclusion at height  $z$  in the true end-annealed brush: (i) We find a lower bound of  $P(z)\Omega$ , closely related to the momentum conservation condition, and corresponding to a fluidized aggregate laterally smeared to infinity; (ii) a shape-dependent upper bound results from a constructed brush configuration correctly respecting incompressibility. For the sphere and cylinder cases the bounds differ only in the prefactor. For the disk, we find an upper bound  $\Delta F < (2/3\pi) P(z)\Omega(l/d)$  which equals our result in the Alexander-de Gennes picture apart from the prefactor. Thus (see fig. 2)

$$\Delta F = \alpha P(z) \Omega \text{ (sphere) , } \quad \Delta F = \beta P(z) \Omega \text{ (cylinder) , } \quad \Delta F = \gamma P(z) \Omega \frac{l}{d} \text{ (disk) , } \quad (3)$$

where  $\alpha, \beta$  are constants and  $1 < \alpha < 5/4$ ,  $1 < \beta < 3/2$ . For the disk we conjecture  $\gamma < 2/3\pi$  is a constant.

We conclude that the effect of end annealing is to replace  $P_0$  with the pressure  $P(z)$  at the aggregate location, and to modify prefactors. Eq. (3) tells us that as nanoparticle aggregates grow their elongation in one lateral direction (cylindrical shape) invokes little penalty,

whereas the brush strongly opposes simultaneous growth in two lateral directions (disk-like) as shown in fig. 2. Macroscopic phase separation within the film is thus suppressed.

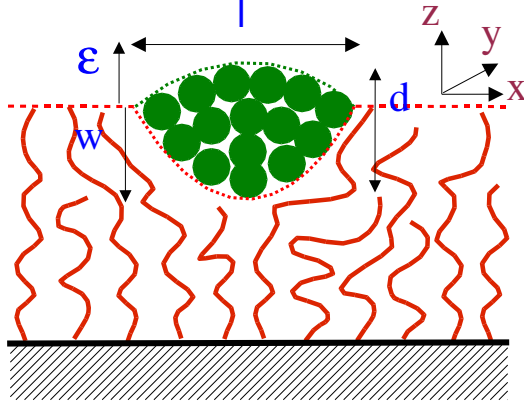


Figure 4: To minimize its free energy a nanoparticle aggregate at the polymer film-air interface chooses a baguette shape of length  $L$  in the  $y$  direction (perpendicular to the plain of the paper). Its cross section comprises 2 half lenses above and below the film surface.

However, due to the  $P(z)$  factors in eq. (3) a “buoyancy” force, strengthening as aggregates grow, thrusts them towards the polymer-air interface. The final state thus hinges on the 3 relevant surface tensions:  $\gamma_{np}$  (nanoaggregate-polymer),  $\gamma_{na}$  (nanoaggregate-air) and  $\gamma_{pa}$  (polymer-air). These determine the familiar *spreading coefficient* [14]  $S \equiv \gamma_{pa} - \gamma_{np} - \gamma_{na}$  and *entry coefficient* [14]  $E \equiv \gamma_{pa} + \gamma_{np} - \gamma_{na}$ . The free energy of a nanoparticle aggregate at the polymer-air interface reads

$$\Delta F = \frac{P_0 L l^3 w^2}{h^3} f_1(L/l) - S L l f_2(L/l) + \left[ \gamma_{na} \frac{L \epsilon^2}{l} + \gamma_{np} \frac{L w^2}{l} \right] f_3(L/l) \quad . \quad (4)$$

Fig. 4 depicts the aggregate of length  $L$  ( $y$  direction) with lens-shaped cross-section of width  $l$  ( $x$  direction) and bulging a depth  $w$  into the brush and  $\epsilon$  into the air ( $\epsilon + w = d$ ). The baguette shape generalizes to anisotropic viscoelastic media the well known result that a droplet on a liquid surface assumes a circular lens shape to minimize its free energy [14]. The first term is the brush stretching energy penalty for a surface depression of depth  $w$ , width  $l$  and length  $L$  [11], the second results from the baguette displacing an area  $Ll$  of air-polymer interface and the last 2 from extra surface area created by each half lens. The factors  $f_i \equiv \alpha_i + \beta_i l/L$  add extra areas due to the baguette’s end-caps (located at  $y = 0, L$ ) where  $\alpha_i, \beta_i$  are constant geometric factors of order unity.

This free energy is somewhat simplified for brevity’s sake (e.g. the baguette may random walk and branch in the  $x$ - $y$  plane) but retains the essential features. Next we minimize the free energy per unit volume for an ensemble of aggregates,  $\Delta F/\Omega$  (where  $\Omega = Lld(A + Bl/L)$  with  $A, B$  constants), subject to the constraint  $\epsilon < \epsilon_{\max}$  where  $\epsilon_{\max}$  is the maximum droplet growth into the air medium allowed by the experimental setup or kinetics (as discussed previously). We find: (i) If  $S > 0$  (i.e. nanoparticles *wet* the polymer material) an infinite nanoparticle monolayer spreads onto the polymer film surface,  $L, l \rightarrow \infty$ ,  $d \rightarrow 0$ . Physically, there is no advantage in penetrating the brush because droplet entry into the polymer-air interface is favored since  $E > 0$  (since  $E > S$  when  $\gamma_{np} > 0$ ). (ii) If  $S < 0$  and  $E > 0$ , we find  $l \approx \delta^{1/4} h$  where  $\delta \equiv \gamma_{np}/P_0 h$  is typically of order unity,  $d$  is also of order  $h$  and  $L \rightarrow \infty$ . That is, nanoaggregates grow freely in one lateral direction, but the brush stabilizes growth in the other lateral direction, selecting a characteristic width. (We find a similar stabilization in the slightly more complex case of  $E < 0$ .)

Let us now compare to experiment. In ref. 5, TEM images of  $2.5nm$  PEP-insoluble (case (B)) dodecanethiol-stabilized gold nanoparticles in PEP thin film brushes show nanoparticles apparently macroscopically phase separated into film surface monolayers, suggesting  $S > 0$ . However,  $5nm$  films exhibited elongated aggregates with a lateral scale of a few  $nm$ , a brush-selected morphology similar to that predicted here. These latter are actually collapsed brushes [5], a case not considered here. We speculate that the thinness of these films prevents wetting and shifts the behavior into the size-stabilized regime described above. Thomas and coworkers [2] report  $4.5nm$  ZnS-coated CdSe particles insoluble (case (B)) in NBPBD-NBP block copolymer films of thickness  $30 - 50nm$  spreading macroscopically on the film surface (fig. 5 of ref. 2). This suggest  $S > 0$  (though loss of the capping species may explain this). But when the solvent was evaporated rapidly, aggregates were instead elongated with finite lateral scale (fig. 6 of ref. 2). This is consistent with a snapshot of the shape-directed aggregate growth kinetics described here. Lauter-Pasyuk et al. [3] studied  $Fe_2O_3$  nanoparticles in lamellar PS-PBMA diblock materials. A corona of PS oligomers apparently rendered particles soluble (case (A)) in the PS domains. Neutron specular reflection data suggested  $6nm$  nanoparticles remain near the PS center plane whilst  $4nm$  particles penetrate further. Tentatively, we estimate  $3.8 \lesssim b^* \lesssim 6.5nm$ , suggesting the partial mixing regime of fig. 3 with the penetration depth  $\delta \sim 1/b^3$  larger for the smaller particles. Balazs and coworkers [4] numerically solved equations describing lamellar diblocks with nanoparticles soluble in one polymer species (case (A)). We estimate  $(b/b^*)$  values of 2 and 1.3, indicating the partial mixing regime (see fig. 3). Consistent with this, nanoparticle density profiles peaked at and decayed away from the lamellar center plane.

In summary, ultrathin films of end-tethered polymers can actively organize nanoparticles to produce novel composite materials. The polymer medium generates effective anisotropic interactions between nanoparticles which direct and stabilize the growth of aggregates within the film and determine the ultimate morphology of the nanoparticle dispersion. The origin of these effects is that the stretching energy cost for polymer brush chains depends strongly on aggregate shape. Our theory suggests two alternative strategies for experimentalists aiming to mix nanoparticles into polymer brushes or lamellar phases. (1) Compatibilize particles to be soluble in the polymer medium and synthesize them as small as possible; particles above a certain size ( $b > b_{max}$ ) will simply not remain within the film. For example, with  $h/R_g = 2$  where  $R_g = N^{1/2}$  is the unperturbed polymer coil size [5] one has  $b_{max} \approx R_g/3 \approx 3nm$  for monomer size  $3nm$  and  $N = 1000$ . (2) To stabilize giant elongated aggregates embedded in the film but near its surface, nanoparticles should be insoluble in the polymer and *non-wetting* on the polymer surface ( $S < 0$ ). Thus, as important as the nanoparticle design is the design of the polymer medium whose incompatibility with air(or whichever is the third medium) should be minimized. Ideally, the polymer should be less incompatible with air than the nanoparticles are ( $\gamma_{pa} < \gamma_{na}$ ): this guarantees a stable morphology.

This work was supported by the MRSEC Program of the NSF, award no. DMR-98-09687. We thank Chris Durning, Rasti Levicky, Royce Murray and Qingbo Yang for stimulating discussions.

## References

- [1] V. Z. -H. Chan *et al.*, Science **286**, 1716 (1999); T. Thurn-Albrecht *et al.*, *ibid.* **290**, 2126 (2000).
- [2] D. E. Fogg *et al.*, Macromolecules **30**, 8433 (1997).
- [3] B. Hamdoun *et al.*, J. Phys. II **6**, 503 (1996); V. Lauter-Pasyuk *et al.*, Physica B **241-243**, 1092 (1998).
- [4] R. B. Thompson *et al.*, Science **292**, 2469 (2001); J. Huh and V. V. Ginzburg and A. C. Balazs, Macromolecules **33**, 8085 (2000).
- [5] Z. Liu, K. Pappacena, J. Cerise, J. Kim, C. J. Durning, B. O'Shaughnessy and R. Levicky, Nanoletters (2002, in press).
- [6] R. W. Zehner *et al.*, Langmuir **14**, 241 (1998); J. F. Ciebien *et al.*, New J. Chem. **22**, 685 (1998); B. Lin *et al.*, J. Appl. Phys. **85**, 3180 (1999).
- [7] P.-G. de Gennes, *Scaling Concepts in Polymer Physics* (Cornell University Press, Itaca and London, 1979).
- [8] A. N. Semenov, Sov. Phys. JETP **61**, 733 (1985).
- [9] In the soluble case, for simplicity we assumed particles are non-wetting on the brush surface ( $S < 0$ ).
- [10] F. J. Solis, Macromolecules **29**, 4060 (1996); F. J. Solis and H. Tang, *ibid.* **29**, 7953 (1996).
- [11] G. H. Fredrickson *et al.*, Macromolecules **25**, 2882 (1992).
- [12] D. R. M. Williams and P. A. Pincus, Europhys. Lett. **24**, 29 (1993).
- [13] H. Lamb, *Hydrodynamics* (Dover Publications, New York, 1945).
- [14] I. Langmuir, J. Chem. Phys. **1**, 756 (1933); P. R. Pujado and L. E. Scriven, J. Colloid Interface Sci. **40**, 82 (1972); R. Aveyard and J. H. Clint, J. Chem. Soc. Faraday Trans. **93**, 1397 (1997).